ADM methodology paper is online

Atmos. Meas. Tech. Discuss., 7, 1–64, 2014
www.atmos-meas-tech-discuss.net/7/1/2014/
doi:10.5194/amtd-7-1-2014

Atmospheric Measurement Techniques Discussions
Open Access

Next-generation angular distribution models for top-of-atmosphere radiative flux calculation from the CERES instruments: methodology

W. Su[1], J. Corbett[2], Z. Eitzen[2], and L. Liang[2]

[1]MS420, NASA Langley Research Center, Hampton, VA 23681, USA
[2]Science Systems & Applications, Inc., Hampton, Virginia, USA

Received: 20 June 2014 – Accepted: 12 August 2014 – Published:

Correspondence to: W. Su (wenying.su-1@nasa.gov)

Published by Copernicus Publications on behalf of the European Geosciences Union.

SW angular distribution model over clear land: Modified RossLi

- Collect clear-sky reflectance over 1°×1° regions for every calendar month;
- Stratify reflectance within each 1°×1° region by NDVI (0.1) and $\cos\theta_0$ (0.2);
- For regions with rough terrain, stratify into two categories;
- Apply modified RossLi fit to produce BRDF and ADM for each NDVI and $\cos\theta_0$ intervals within each 1°×1° region.

$$\rho(\mu_0, \mu, \phi) = k_0 + k_1 \cdot B_1(\mu_0, \mu, \phi) + k_2 \cdot B_2(\mu_0, \mu, \phi)$$

from Maignan et al., 2004

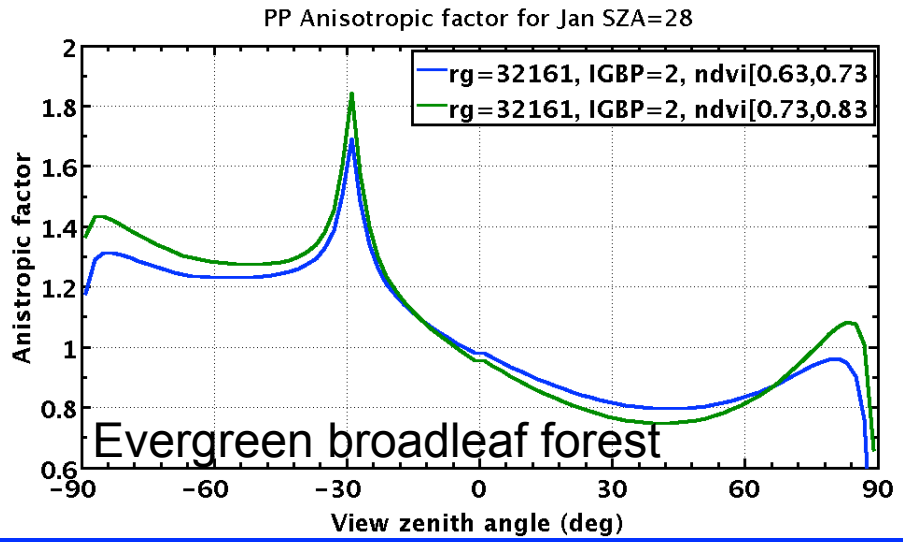

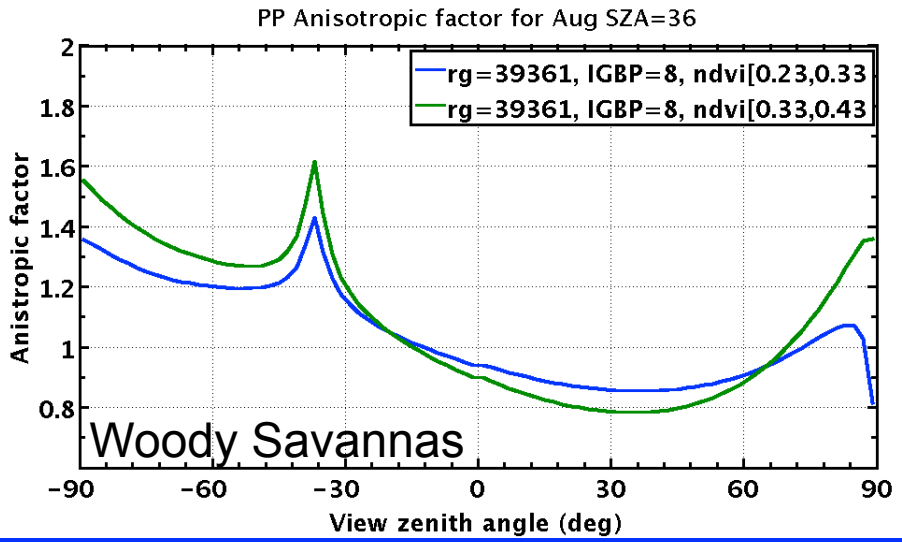

Ed4ADM over clear ocean accounts for aerosol loading and type

- AOD retrieval based upon a fine-mode aerosol look-up table (urban) and a coarse-mode aerosol look up table (maritime);
- Stratify fine-mode aerosols into 3 AOD bins and coarse-mode aerosols into 3 AOD bins;
- Build ADM for each AOD bin and type separately (6 ADMs).

$$\epsilon_c = \sum_{j=1}^{6}$$

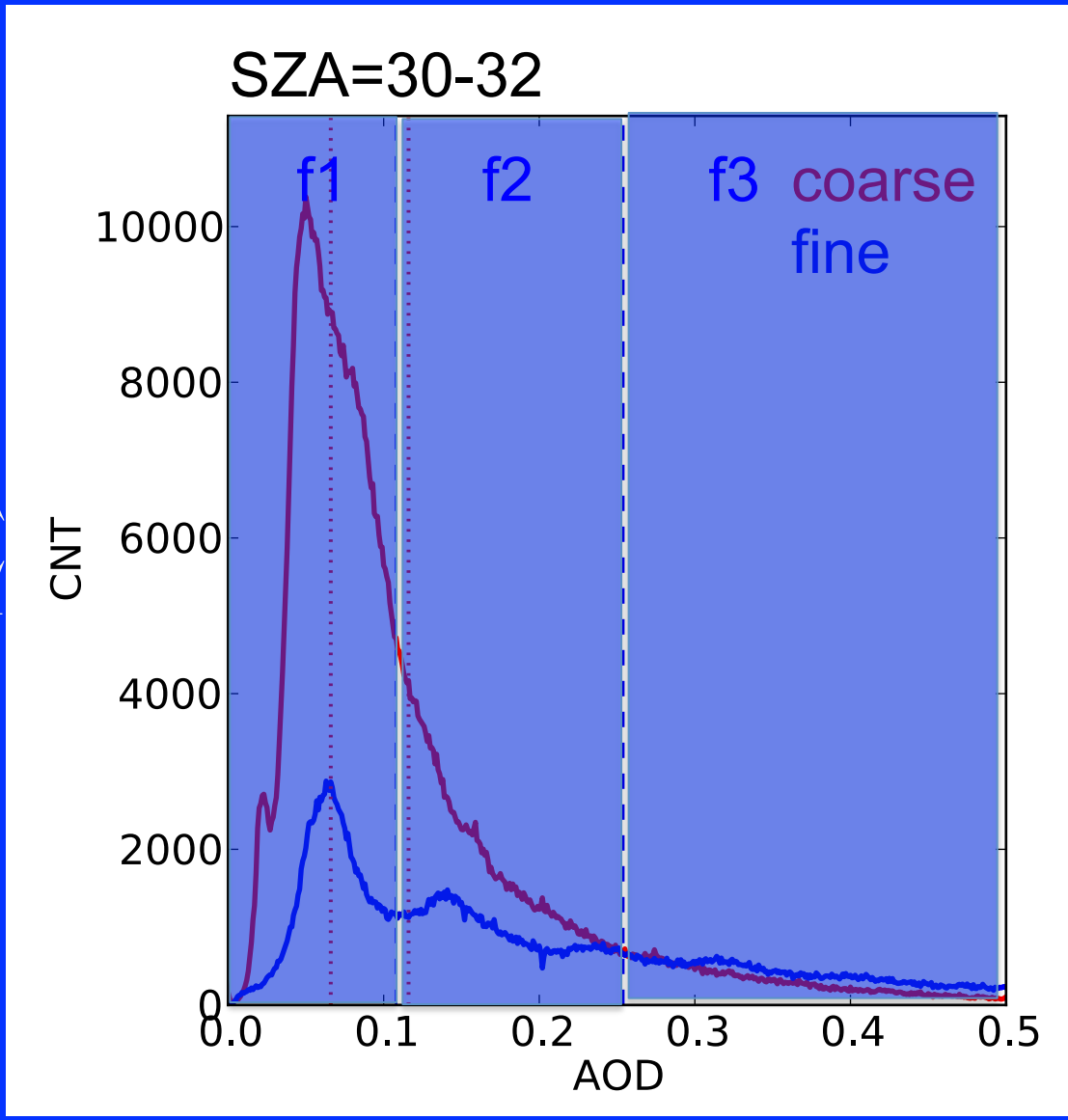

Sea ice index to quantify the brightness of sea ice surface

$$\eta = 1 - \frac{\rho_{0.47} - \rho_{0.86}}{\rho_{0.47} + \rho_{0.86}}$$

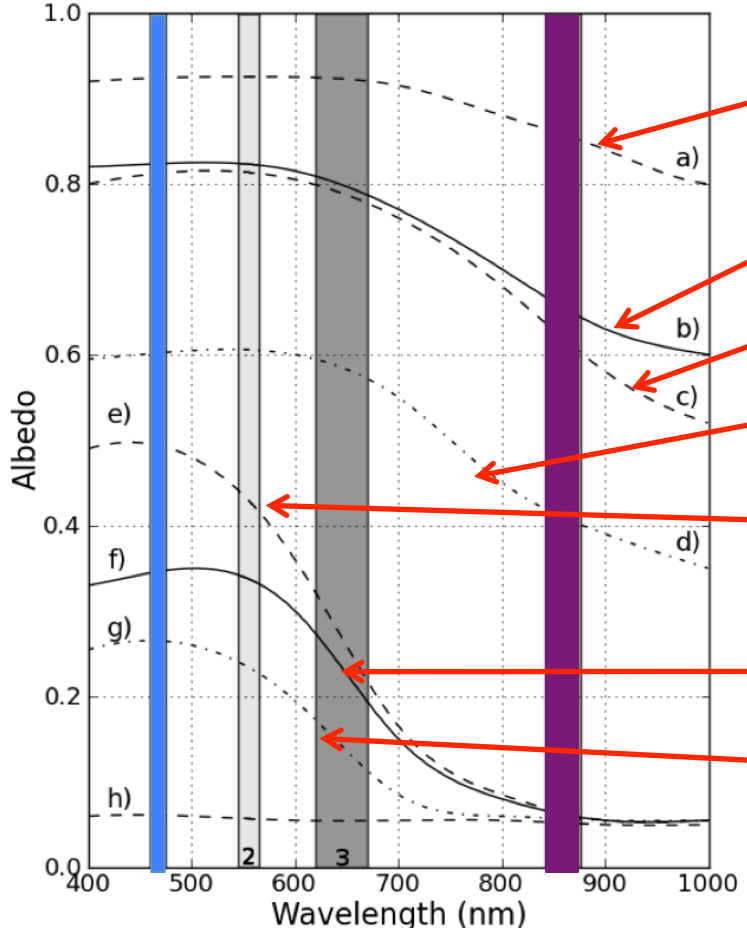

Rosel et al 2012, surface values

High sea ice index

Snow

Bare ice

Wet snow

Melting first year ice

~0.8-1.0

Young melting pond

Melt ponds

Open water

~0.1-0.5

Low sea ice index

Sea ice index decreases as ice starts melting

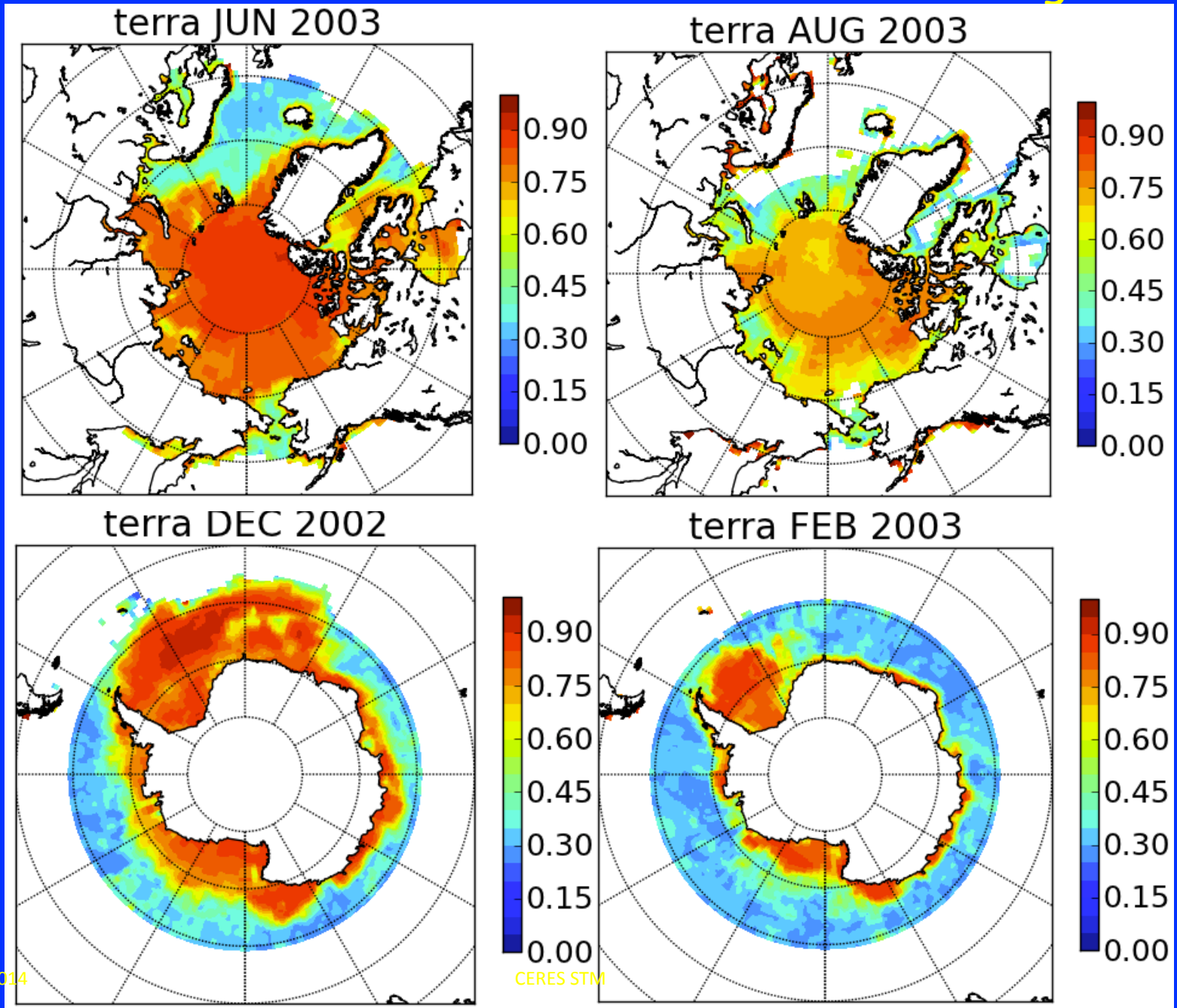

Regional TOA SW flux uncertainties: direct integration

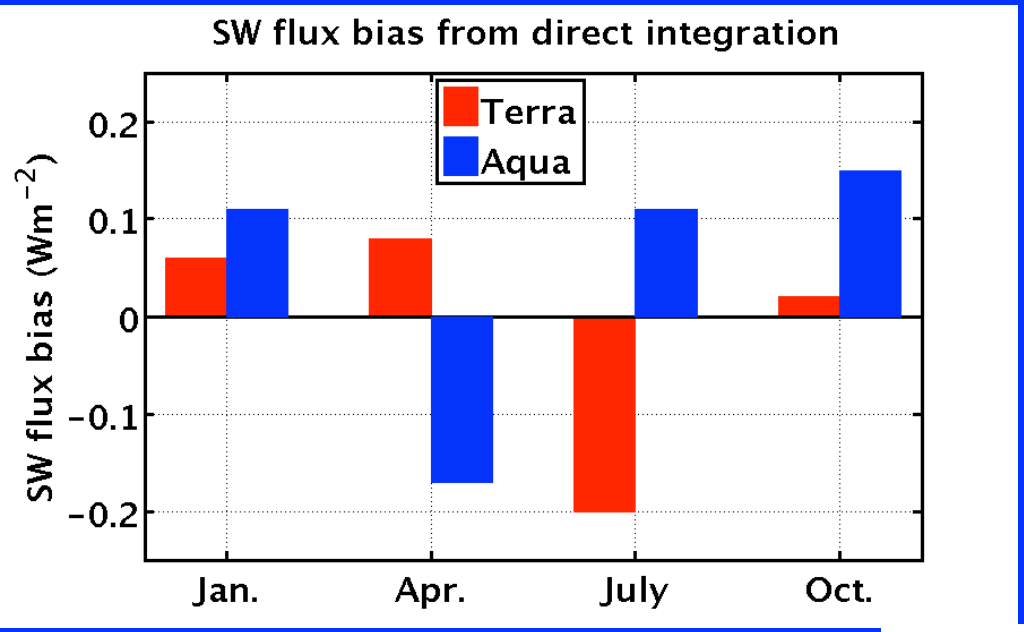

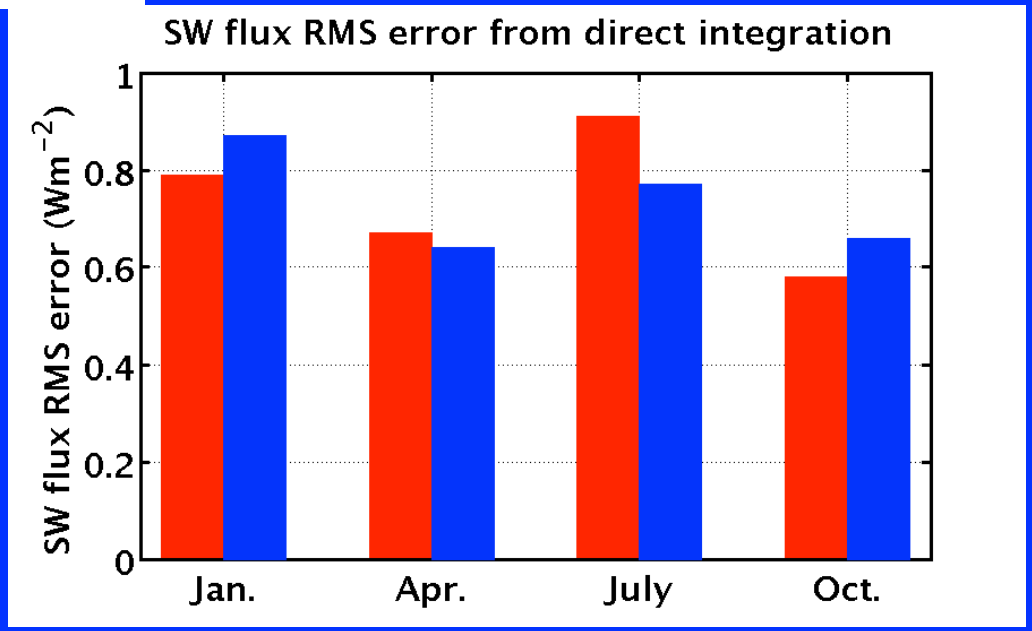

Regional TOA LW flux uncertainties: direct integration

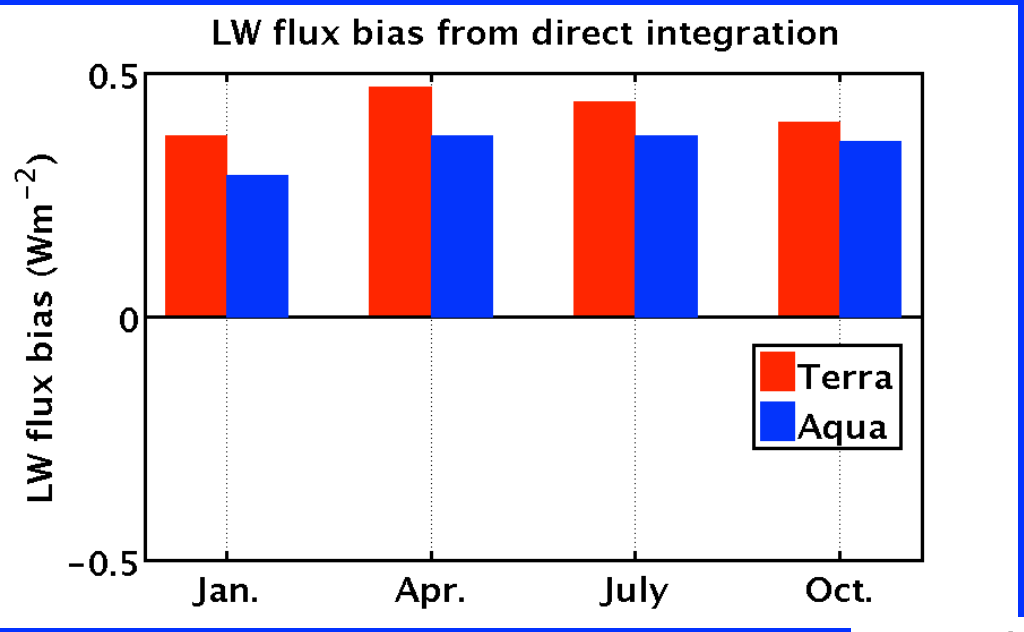

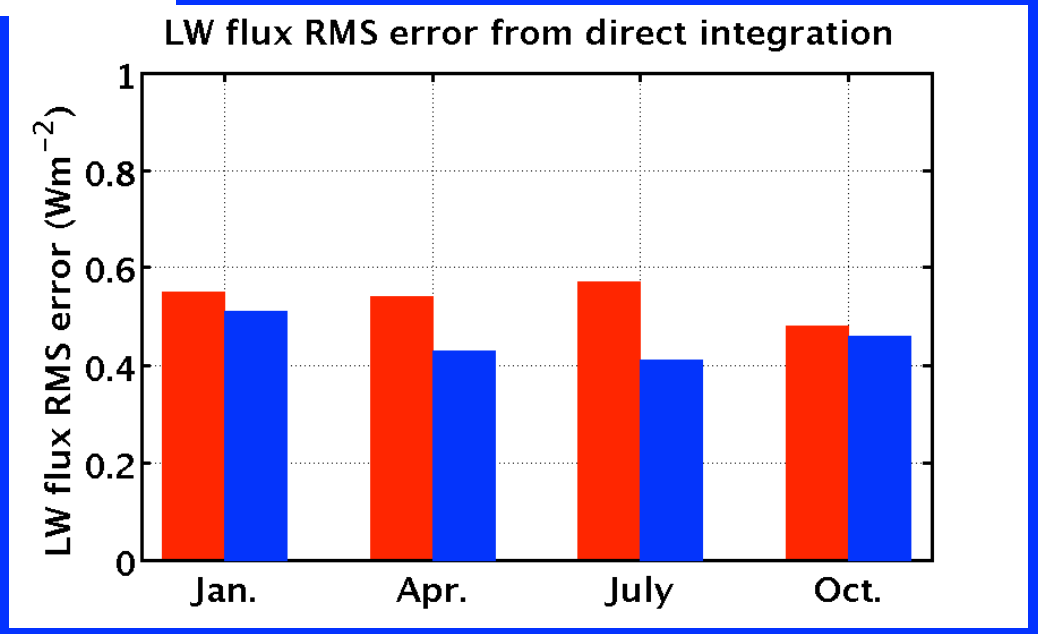

CERES-MODIS instantaneous TOA flux consistency test

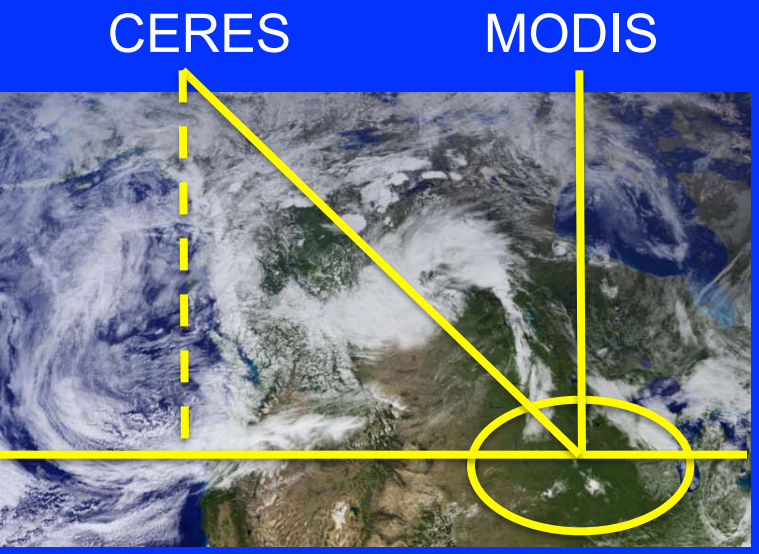

$$I_{sw}^{c} \qquad I_{sw}^{md} = d_0 + d_1 I_{0.65} + d_2 I_{0.86} + d_3 I_{1.63}$$

$$I_{lw}^{c} \qquad I_{lw}^{md} = \alpha_0 + \alpha_1 I_{11}$$

CERES ADM

$$F(\theta^o) \qquad F(\theta^n)$$

$$\sigma = \sqrt{\frac{1}{N}\sum_{i=1}^{N}\left[F(\theta_i^n) - F(\theta_i^o)\right]^2}$$

Instantaneous flux bias and RMS error determined from CERES-MODIS consistency test

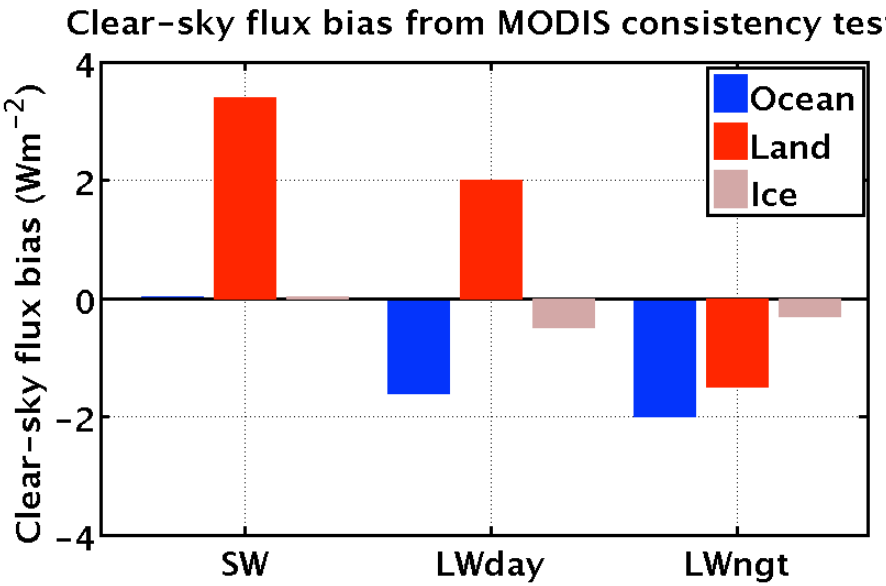

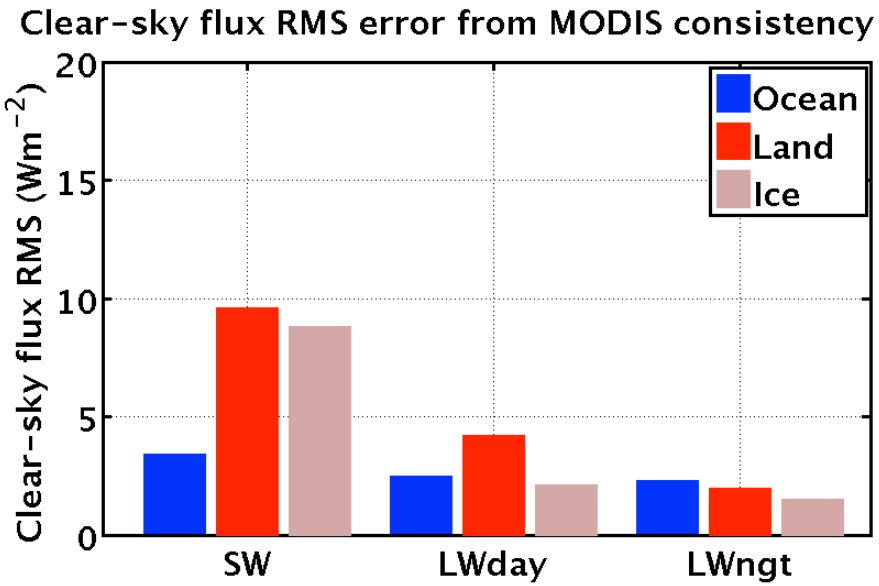

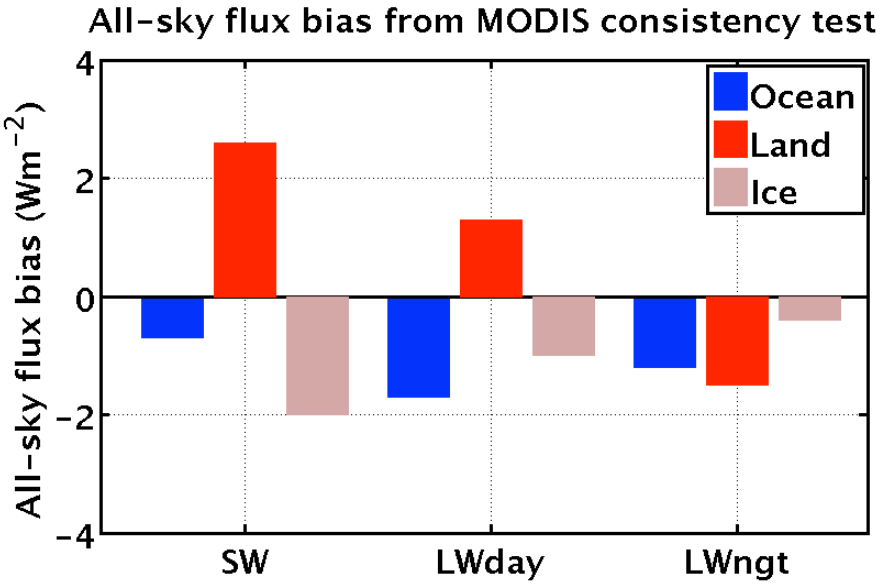

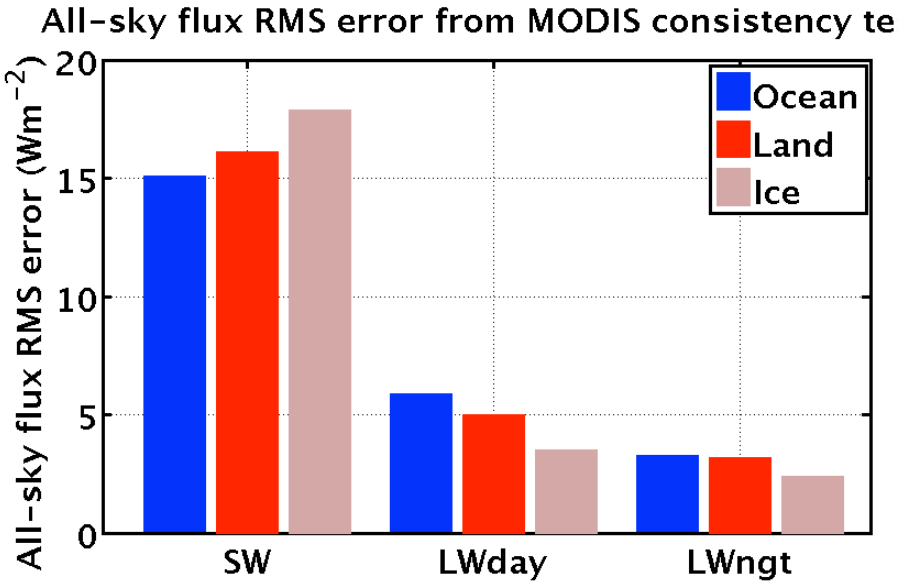

Flux uncertainty from scene identification error

- CALIPSO, CERES, CloudSat, and MODIS (C3M) product provides coincident
  - "standard" CERES-MODIS cloud property retrievals over the CALIPSO/CloudSat ground track
  - "enhanced" cloud property retrievals using cloud height from CALIPSO/CloudSat as input to the "standard" algorithm
- Assuming "enhanced" C3M cloud properties are the truth, and the CALIPSO ground track observation is representative of the whole CERES footprint
- We select the anisotropic factors based upon scene identification provided by the "standard" algorithm and the "enhanced" algorithm, the flux difference is attribute to scene identification error

CERES-MODIS standard cloud algorithm underestimates cloud effective height compared to the enhanced cloud algorithm

Day

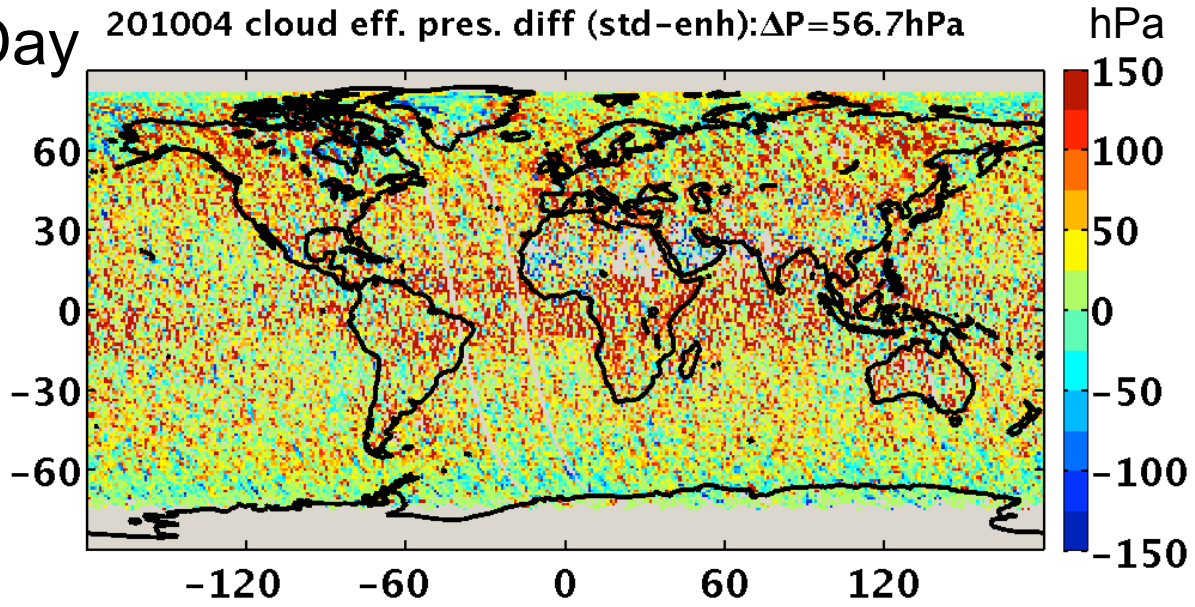

Night

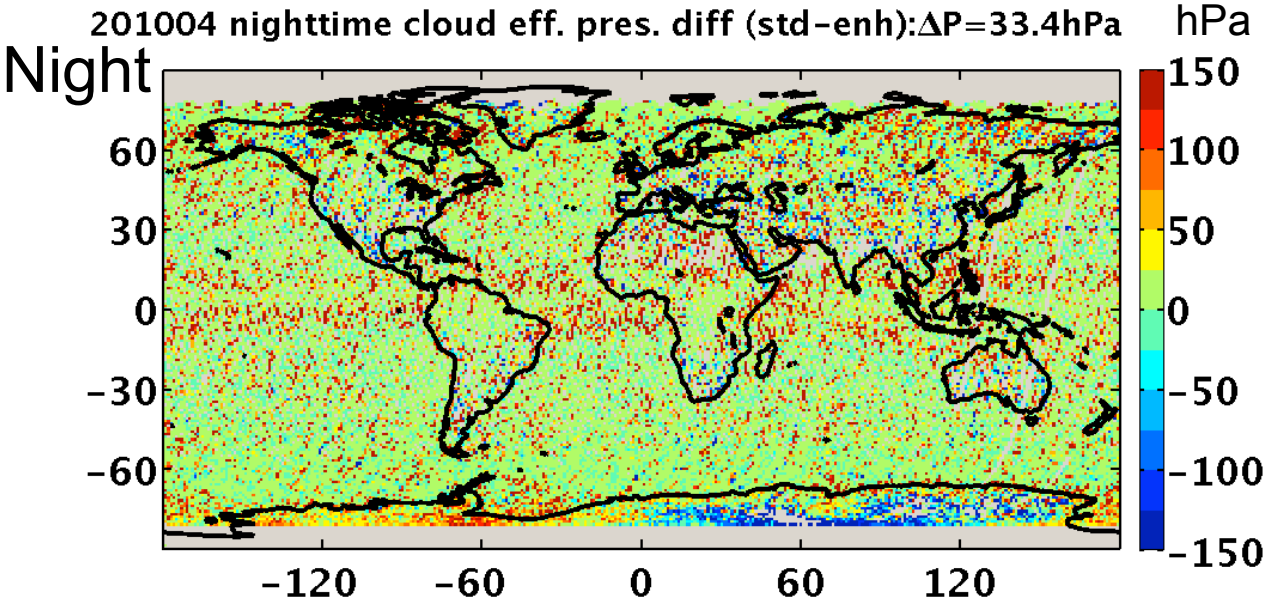

CERES-MODIS standard cloud algorithm underestimates cloud compared to the enhanced cloud algorithm

Day

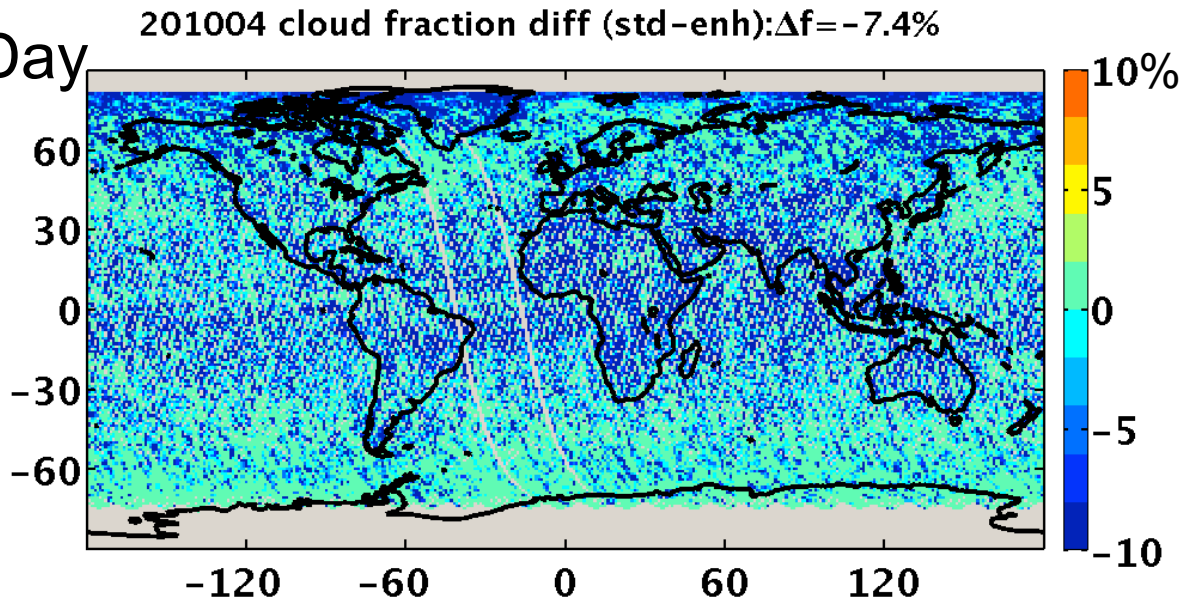

Night

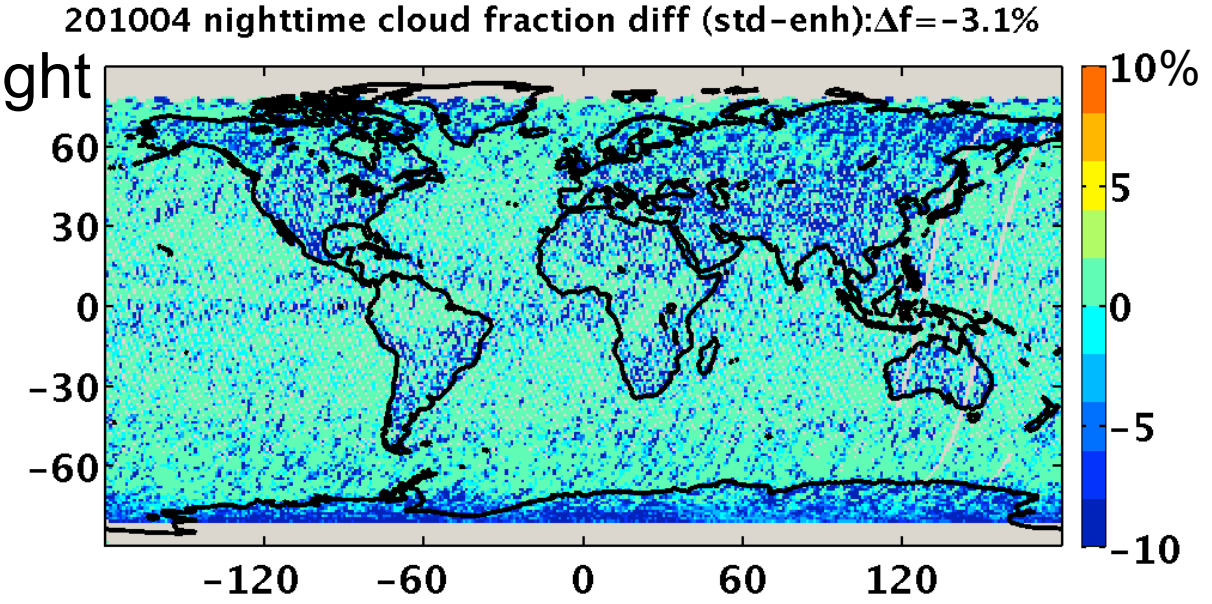

CERES-MODIS standard cloud algorithm overestimates cloud optical depth compared to the enhanced cloud algorithm

Day

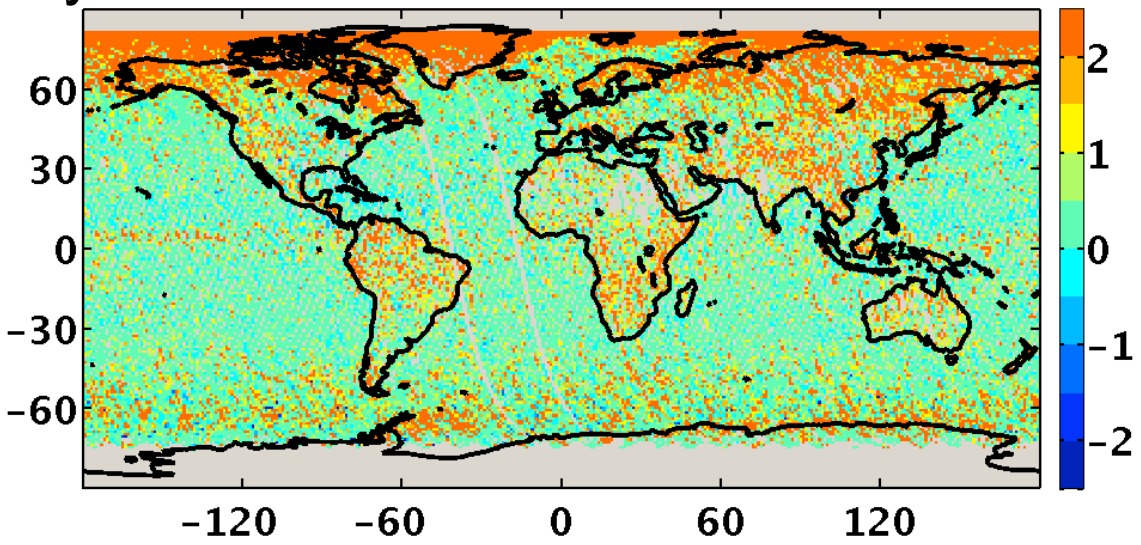

Night

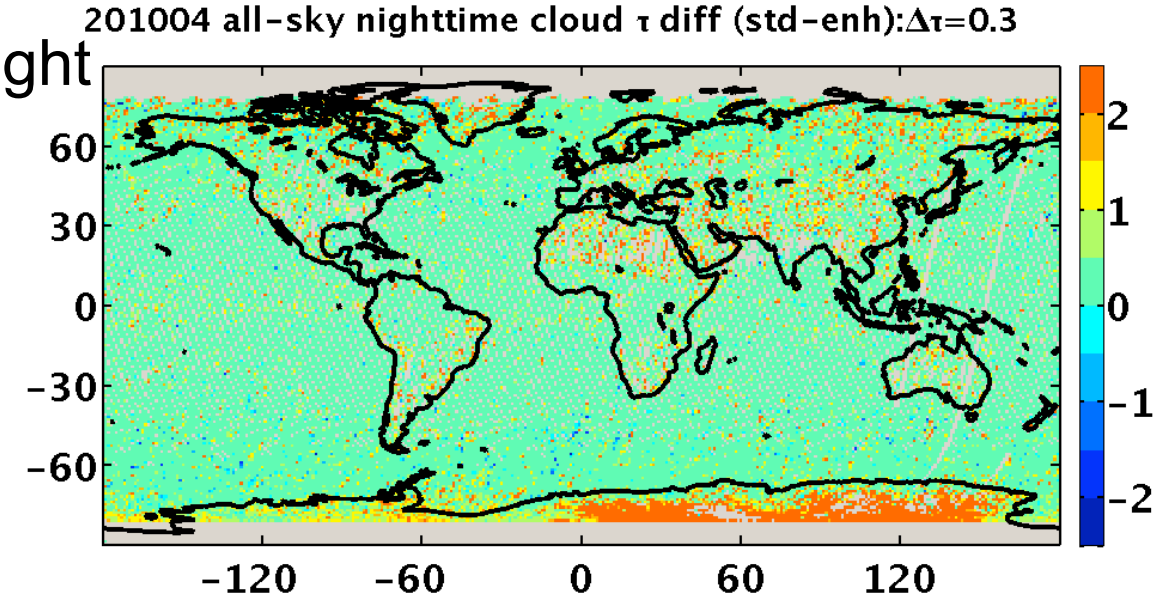

SW flux is underestimated and LW flux is overestimated due to scene identification error

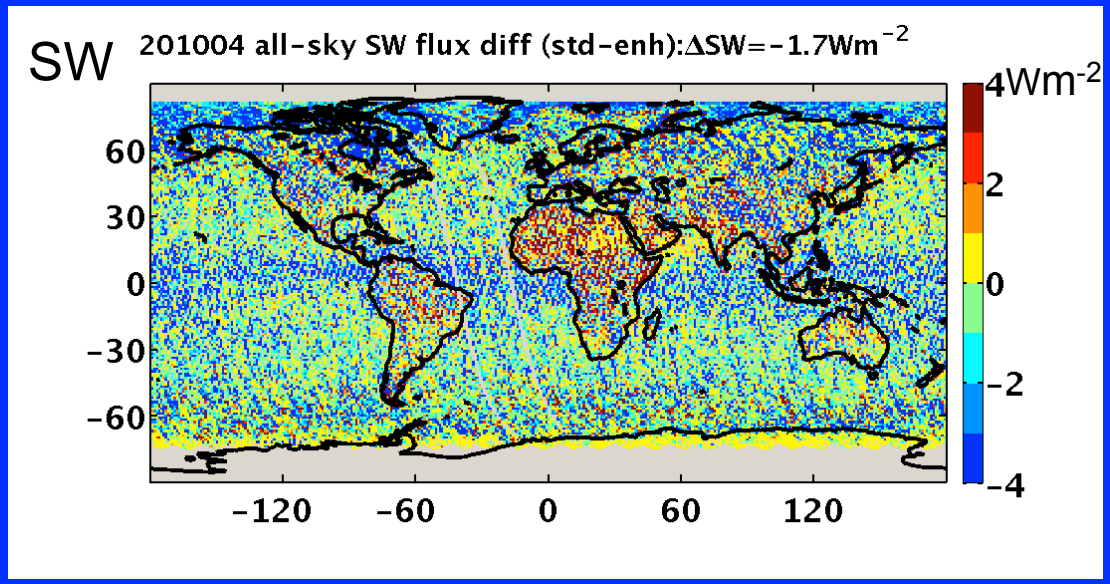

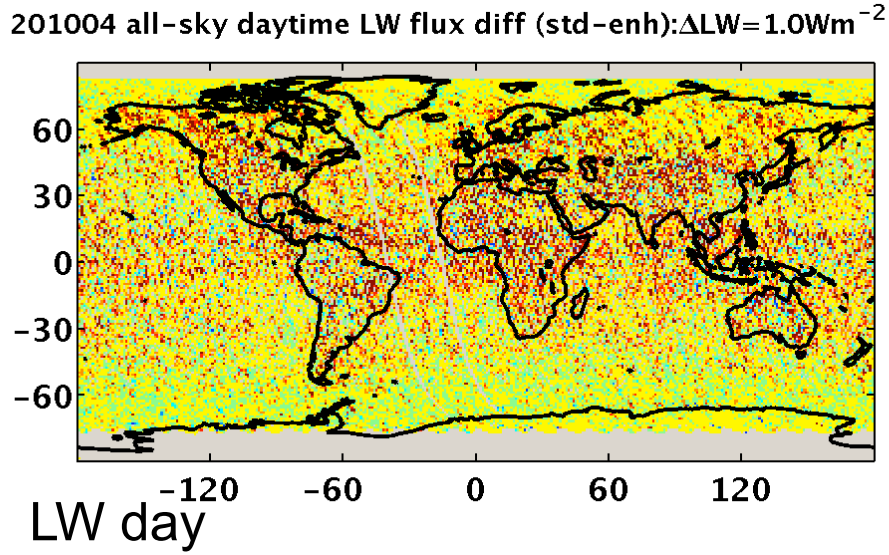

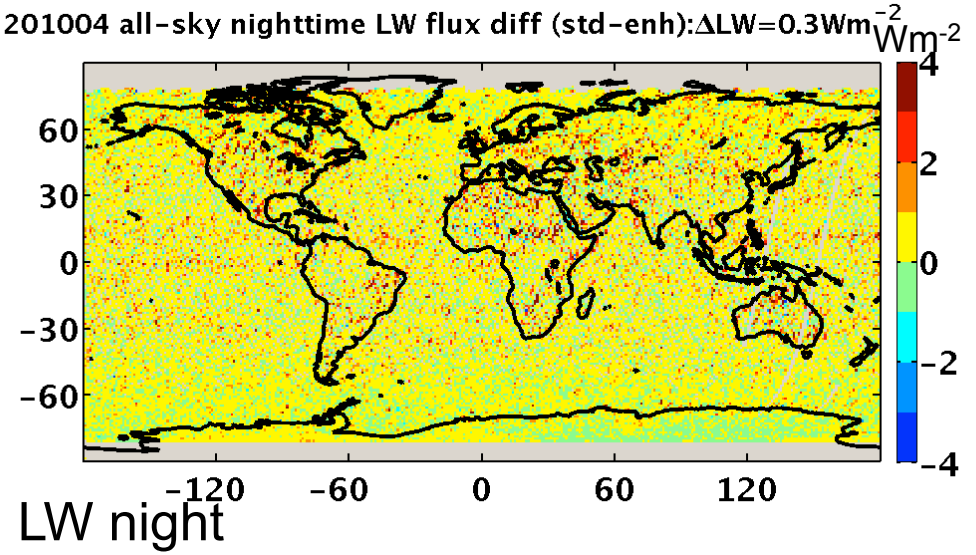

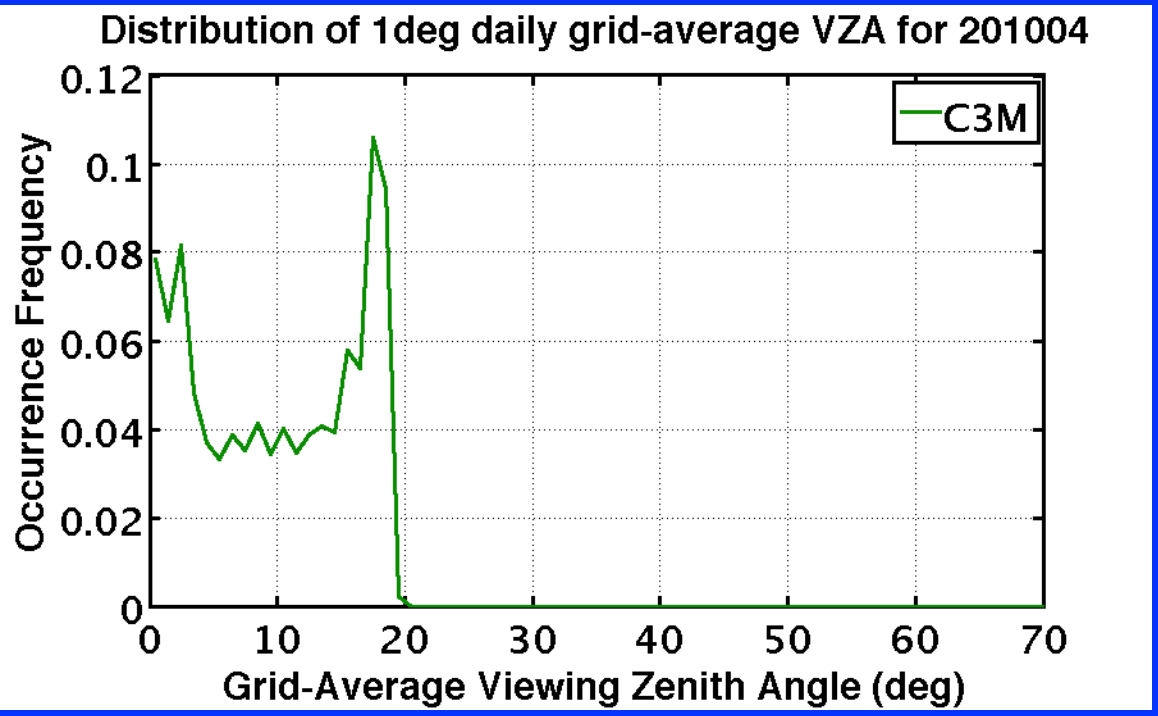

CERES footprints in the C3M product are all near-nadir viewing footprints

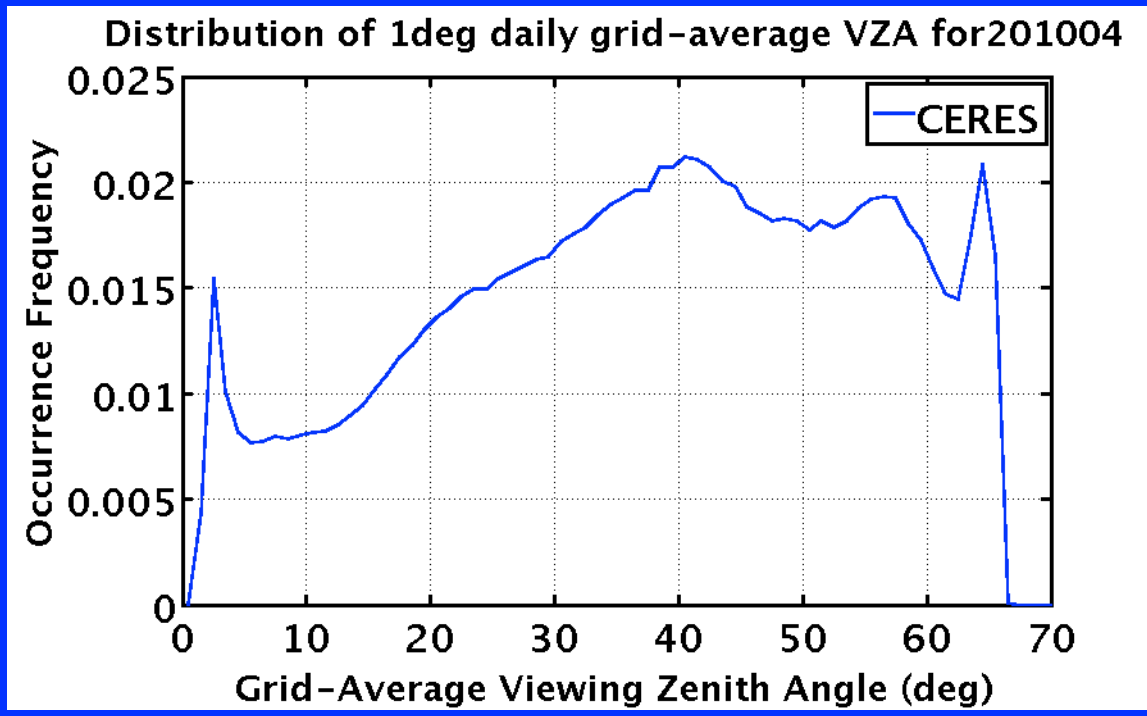

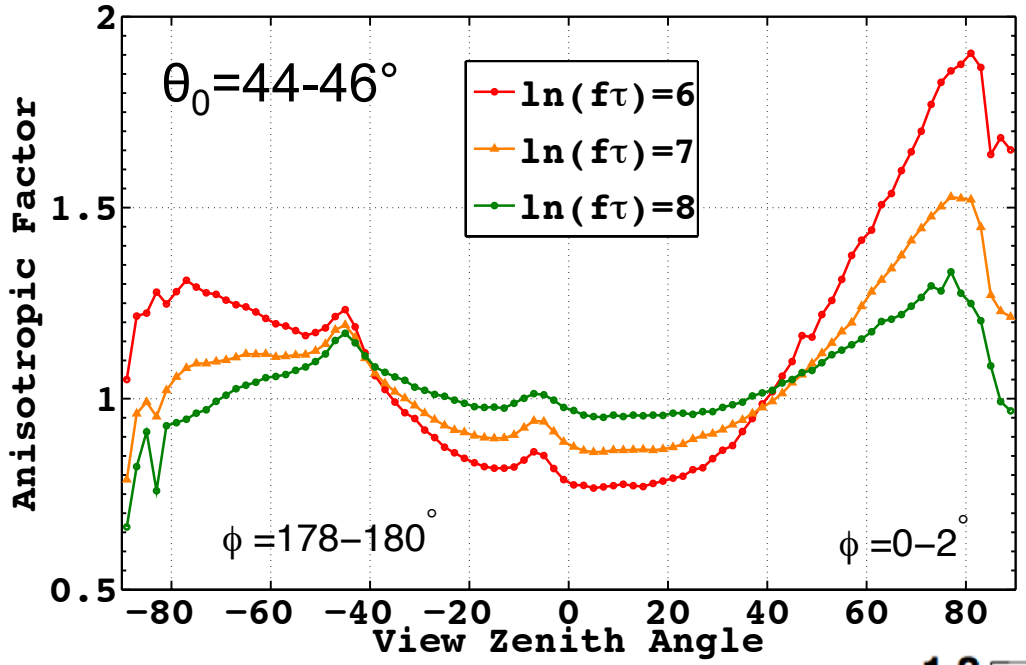

Anisotropic factors depend on viewing zenith angle

$$F(\theta_0) = \frac{\pi I_o(\theta_0, \theta, \phi)}{R(\theta_0, \theta, \phi)}$$

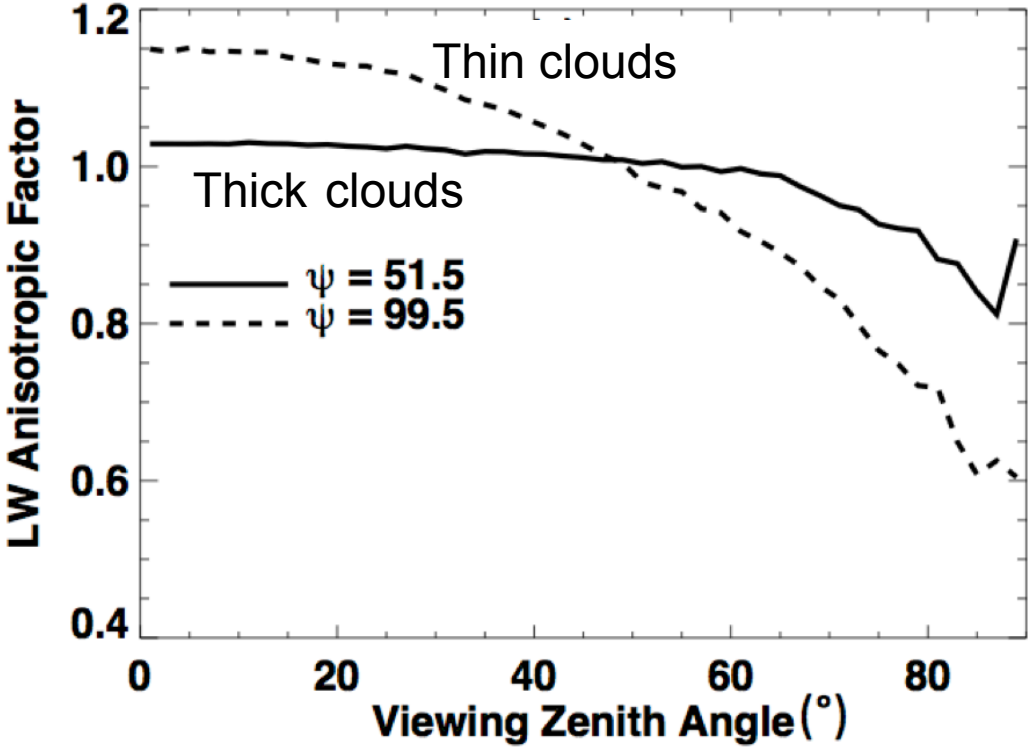

Extend the near-nadir viewing only comparison to 'real' CERES viewing geometries

- Assuming the near-nadir viewing cloud property differences between "standard" algorithm and "enhanced" algorithm are representative for the whole CERES swath (~24° longitude bins).
- Repeating the flux calculation using all sun-viewing geometries sampled by CERES for each 0.2° latitude by 24° longitude bin for each day.
- The 0.2° latitude by 24° longitude produces the most realistic PDFs of the daily grid-average viewing zenith angle.

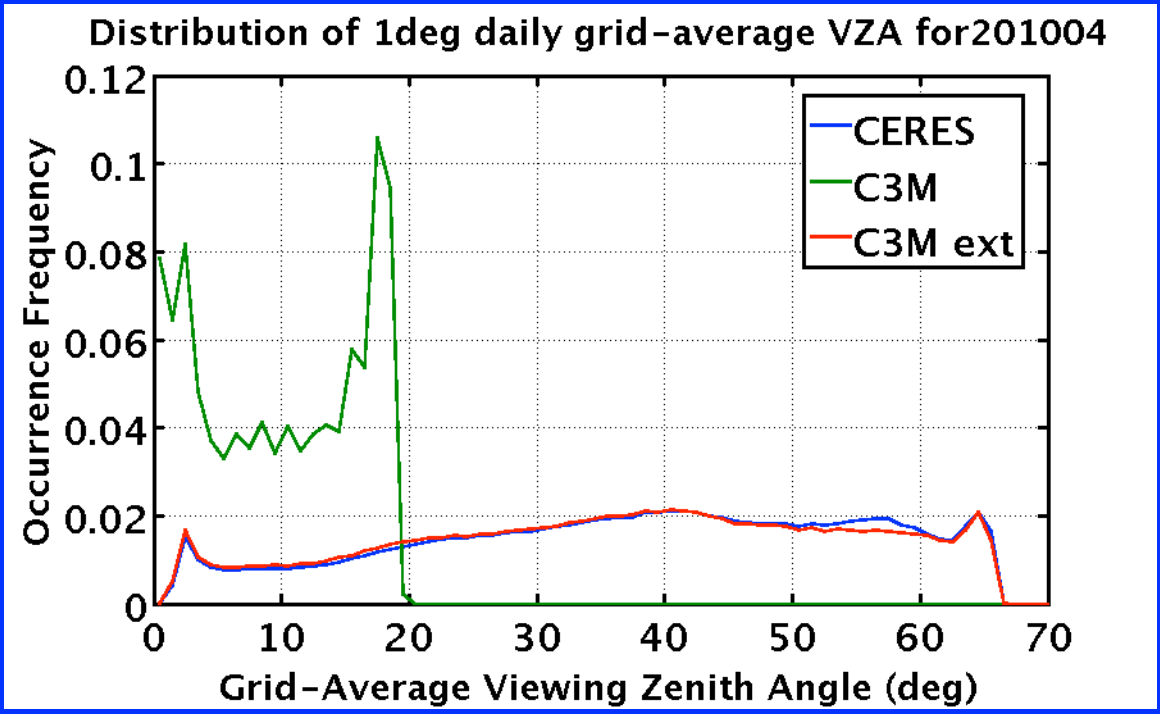

Extending the viewing geometry reduces the SW flux difference by 1Wm^{-2}

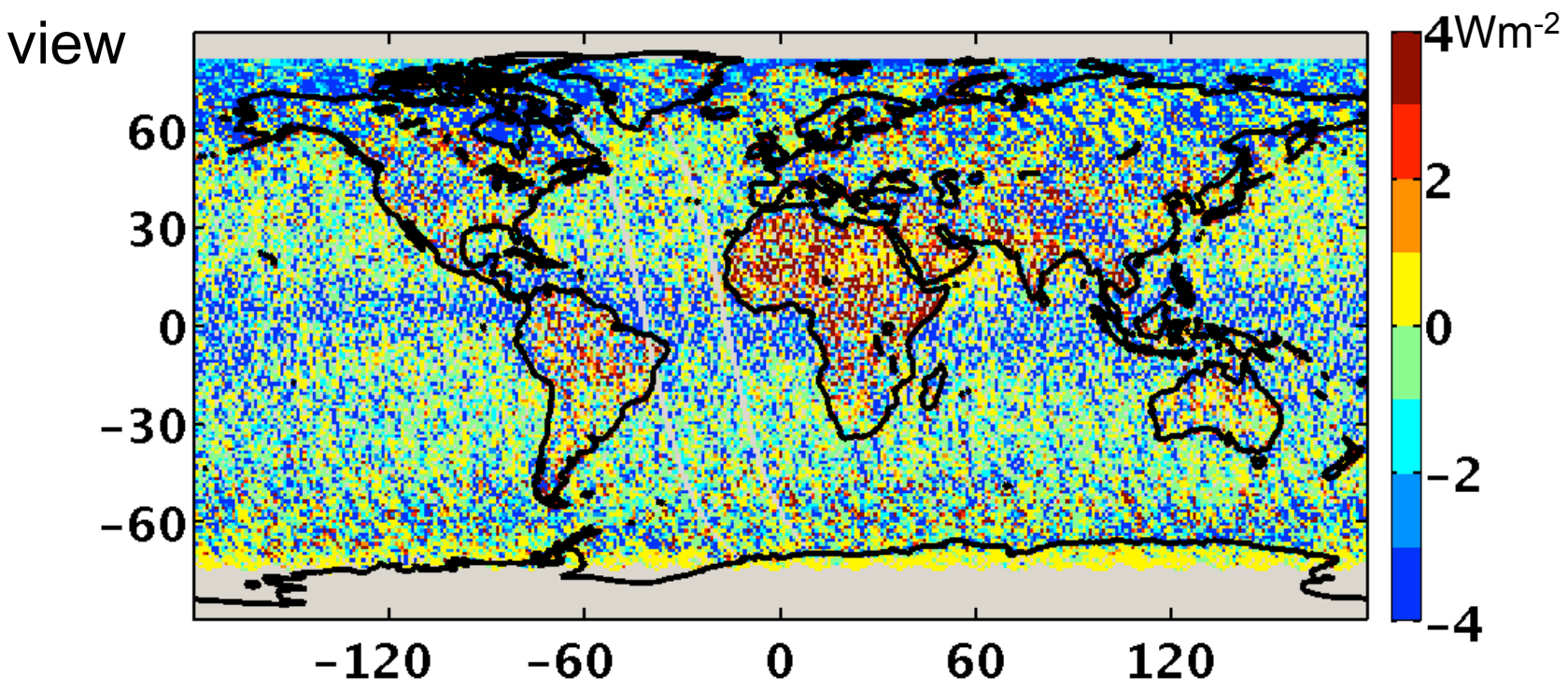

Summary

- CERES TOA SW flux uncertainties
  - global mean uncertainty is less than 0.2 Wm^{-2}
  - Instantaneous uncertainty is 15~18 Wm^{-2}
- CERES TOA LW flux uncertainties
  - global mean uncertainty is less than 0.4 Wm^{-2}
  - Instantaneous uncertainty is 3~6 Wm^{-2}
- Flux uncertainty from scene identification using near-nadir footprints
  - SW is underestimated by 1.6 to 1.8 Wm^{-2}
  - LW daytime is overestimated by 0.8 to 1.0 Wm^{-2}
  - LW nighttime is overestimated by 0.3 Wm^{-2}
- Flux uncertainty from scene identification using CERES sun-viewing geometry
  - SW is underestimated by 0.5 to 0.7 Wm^{-2}